Aust. J. Phys., 2000, **53**, 3–34

Monte Carlo Investigation of Shot-noise Suppression in Nondegenerate Ballistic and Diffusive Transport Regimes*

L. Reggiani,[A] *A. Reklaitis,*[B] *T. González,*[C] *J. Mateos,*[C] *D. Pardo*[C] *and O. M. Bulashenko*[D]

[A] Istituto Nazionale di Fisica della Materia,
Dipartimento di Ingegneria dell' Innovazione,
Università di Lecce, Via Arnesano, 73100 Lecce, Italy.
[B] Semiconductor Physics Institute, Goshtauto 11,
2600 Vilnius, Lithuania.
[C] Departamento de Física Aplicada, Universidad de Salamanca,
Plaza de la Merced s/n, E-37008 Salamanca, Spain.
[D] Departament de Física Fonamental, Universidad de Barcelona,
Av. Diagonal 647, E-08028 Barcelona, Spain.

Abstract

We review recent theoretical investigations of shot-noise suppression in nondegenerate semiconductor structures surrounded by two contacts acting as thermal reservoirs. Calculations make use of an ensemble Monte Carlo simulator self-consistently coupled with a one-dimensional Poisson solver. By taking the doping of the injecting contacts and the applied voltage as variable parameters, the influence of elastic and inelastic scattering as well as of tunneling between heterostructures in the active region is investigated. In the case of a homogeneous structure at $T = 300$ K the transition from ballistic to diffusive transport regimes under different contact injecting statistics is analysed and discussed. Provided significant space-charge effects take place inside the active region, long-range Coulomb interaction is found to play an essential role in suppressing shot noise at applied voltages much higher than the thermal value. In the elastic diffusive regime, momentum space dimensionality is found to modify the suppression factor γ, which within numerical uncertainty takes values respectively of about $\frac{1}{3}$, $\frac{1}{2}$ and $0{\cdot}7$ in the 3D, 2D and 1D cases. In the inelastic diffusive regime, shot noise is suppressed to the thermal value. In the case of single and multiple barrier non-resonant heterostructures made by GaAs/AlGaAs at 77 K, the mechanism of suppression is identified in the carrier inhibition to come back to the emitter contact after having been reflected from a barrier. This condition is realised in the presence of strong inelastic scattering associated with emission of optical phonons. At increasing applied voltages for a two-barrier structure, shot noise is suppressed up to about a factor of $0{\cdot}50$ in close analogy with the corresponding resonant barrier-diode. For an increasing number of barriers, shot noise is found to be systematically suppressed to a more significant level by following approximately a $1/(N+1)$ behaviour, N being the number of barriers. This mechanism of suppression is expected to conveniently improve the signal-to-noise ratio of these devices.

1. Introduction

Electronic noise manifests itself in the stochastic behaviour of the stationary current as measured in the outside circuit of a two-terminal device under test

* Refereed paper based on a talk presented to the Workshop on Nanostructures and Quantum Confinements, held at the Australian National University, Canberra, in December 1998.

10.1071/PH99034 0004-9506/00/010003$10.00

when biased with a constant voltage (current-mode operation), as schematically shown in Fig. 1. Noise is a key feature of any electronic device because it gives the intrinsic limit of the performance defined by the signal-to-noise ratio figure of merit. However, besides hindering the signal detection, noise is also a relevant probe of the microscopic phenomena at hand, thus providing information not otherwise available from the study of average quantities, like conductance. When moving toward nanostructures new phenomena have been found to arise and innovative concepts need to be introduced (de Jong and Beenakker 1996). This is the case for shot noise and its suppression, which has emerged in recent years as a very interesting phenomenon not yet fully understood.

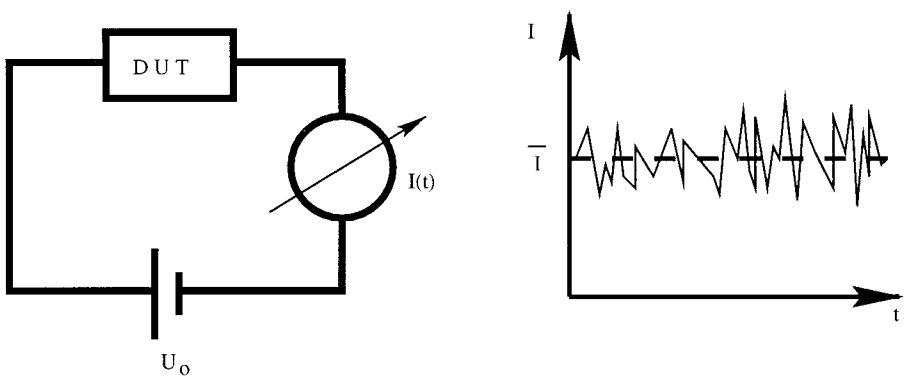

Fig. 1. Schematic drawing of a two-terminal device under test (DUT) in which a stationary fluctuating current is flowing under constant voltage conditions.

The aim of this paper is to overview recent Monte Carlo (MC) investigations of shot-noise suppression we have carried out in two-terminal structures of small dimensions (i.e. with typical submicrometre length scale) undergoing electronic transport ranging from the ballistic to diffusive regime (here ballistic and diffusive are synonymous with the absence or presence of scattering respectively). We consider separately the cases when transport is dominated by scattering only and when it is mostly controlled by tunneling processes. The MC simulations refer only to nondegenerate conditions, and the applied voltage U is allowed to be sufficiently high so that the device can strongly depart from ohmic conditions (i.e. linear current–voltage characteristics). Furthermore, the phonon bath is assumed to remain at thermal equilibrium. The main objectives are to analyse separately the effects of (i) scattering (elastic and inelastic), (ii) tunneling, (iii) space-charge, and (iv) carrier injection modeling from the contacts, on shot noise and its suppression. The degenerate conditions have been already widely investigated and, for the sake of completeness, a brief survey of the existing literature is reported.

The paper is organised as follows. In Section 2 we recall the general definitions and properties of current fluctuations. Section 3 briefly reviews the phenomenon of shot-noise suppression providing an up-to-date state of the art summary. The theoretical model used in MC calculations is given in Section 4. Section 5 displays the results for the two main structures considered here namely: the homojunction and the tunneling heterojunction structures. Section 6 summarises the main conclusions.

2. Current Fluctuations: General Definitions and Properties

With reference to Fig. 1*a*, the general physical system under investigation is a two-terminal device in which a stationary fluctuating current $I(t)$ is flowing as a result of an applied bias constant in time. Ideal leads connecting the device to the applied voltage are implicitly assumed, so that the current is determined only by the characteristics of the device under test. By introducing the current fluctuation $\delta I(t) = I(t) - \bar{I}$, the main quantity of interest which provides a theoretical description of noise is the correlation function of current fluctuations, defined as

$$C_I(t) = \tfrac{1}{2}[\overline{\delta I(0)\delta I(t)} + \overline{\delta I(t)\delta I(0)}]\,, \tag{1}$$

where stationary conditions imply translation invariance in time of the correlator, the bar denotes time (or ensemble) average by assuming ergodicity, and a symmetrised notation has been introduced to generalise the description to the quantum case when dynamic variables are replaced by corresponding operators.

In the frequency domain (typical of the experimental detection of noise) the counterpart of the correlation function is the spectral density of current fluctuations $S_I(f)$, defined as:

$$S_I(f) = 2\int_{-\infty}^{+\infty} C_I(t)\exp(i2\pi ft)dt\,. \tag{2}$$

The noticeable property of the spectral density is to satisfy the power theorem which relates the variance of current fluctuations $\overline{\delta I^2}$ to the spectrum as

$$\overline{\delta I^2} = \int_0^{\infty} S_I(f)df\,. \tag{3}$$

We remark that an analogous (or dual) representation of noise can be given for voltage fluctuations as measured at the open terminals of the device under test. Because of the linearity of the fluctuations we are concerned with, the Norton/Thevenin circuit theorems relate voltage and current spectra as (van der Ziel 1954)

$$S_U(f)/S_I(f) = |Z(f)|^2\,, \tag{4}$$

where $Z(f)$ is the small signal impedance of the device under test. We recall the relation $Z(f) = 1/Y(f)$ where $Y(f)$ is the small signal admittance of the device.

Since electronic noise is already present at thermal equilibrium due to the coupling of the device with the environment (thermal reservoir), it is convenient to introduce the concept of *excess* noise defined as the contribution which algebraically adds to that already present under thermal equilibrium. We remark that the microscopic sources of excess noise differ in general from that of the thermal one. Examples of excess noise are: $1/f$ or flicker noise, generation recombination noise, hot-carrier noise, shot noise, etc.

(2a) Thermal Noise

Thermal noise is associated with the thermal coupling of carriers with the environment. It is always present and is rigorously described under thermal equilibrium conditions by the Nyquist theorem which, in its quantum form, gives the well known relationship (Kubo *et al.* 1991)

$$S_I^{\mathrm{Th}}(f) = 4\mathrm{Re}[Y(f)]\ hf\ \coth\left(\frac{hf}{2KT}\right), \tag{5}$$

where the superscript Th emphasises the thermal source of fluctuations, $\mathrm{Re}[Y(f)]$ is the real part of the small signal admittance of the device at frequency f, h is the Planck constant, K the Boltzmann constant and T the absolute temperature.

In particular, for a space homogeneous device (conductor), by using the Einstein relation at zero frequency, we have

$$S_I^{\mathrm{Th}}(0) = 4KTG = \frac{4q^2}{L^2} D\overline{\delta N^2}, \tag{6}$$

with G the static conductance, q the electron charge, L the length of the conductor, D the diffusion coefficient and $\overline{\delta N^2}$ the variance of the number of carriers inside the conductor, given by the grand canonical relation (Landau and Lifshitz 1958)

$$\overline{\delta N^2} = \bar{N} KT \frac{\partial \ln \bar{N}}{\partial \mu_0}, \tag{7}$$

μ_0 being the chemical potential.

The following are remarkable properties of thermal noise:

(i) under nondegenerate conditions $\overline{\delta N^2} = \bar{N}$ and, for $T \to 0$, $D \to 0$; thus noise and diffusion are synonymous.

(ii) under degenerate conditions for $T \to 0$, $\overline{\delta N^2} \to 0$ and $D \neq 0$; thus in general noise is related to the product of diffusion and variance of carrier number fluctuations, evidence of the open system characteristics.

(iii) thermal noise does not depend on the discreteness of the charge; i.e. by halving the charge unit and mass and doubling the carrier number the conductance remains the same and thus also the current spectral density.

(iv) it is rigorously defined at thermodynamic equilibrium (fluctuation-dissipation theorem), and its zero frequency value vanishes at $T = 0$, a zero-point contribution is present at finite frequencies.

(v) the frequency dependence of the spectrum $S_I(f)$ is a fingerprint of carrier dynamics, and for a relaxation regime it takes a Lorentzian shape.

(2b) Shot Noise

Shot noise is associated with the discreteness of electrical charge. The standard device exhibiting shot noise is the vacuum diode. Here shot noise is associated with the fluctuations of the total number of carriers inside the device as a consequence of the random injection from the cathodic contact, and is given by the well-known formula

$$S_I^{\mathrm{Sh}}(0) = 2q\bar{I}\ \gamma\,, \tag{8}$$

where the superscript Sh emphasises the shot-noise characteristics of fluctuations, q is the unit of charge responsible for the current (not necessarily equal to the electron charge) and γ is the suppression (or Fano) factor. The suppression factor is a measure of the correlation between different current pulses crossing the device and it can take the following range of values:

$\gamma = 1 \rightarrow$ full shot noise (absence of correlations);

$\gamma < 1 \rightarrow$ suppressed shot noise (negative correlations);

$\gamma > 1 \rightarrow$ enhanced shot noise (positive correlations).

The following are remarkable properties of shot noise:

(i) it is an excess noise and thus it vanishes in the absence of a driving field.
(ii) it linearly scales with the value of the quantum of charge responsible for the current.
(iii) the frequency dependence of the spectrum $S_I(f)$ is a fingerprint of carrier dynamics.

We point out that we reject the recurrent interpretation of thermal noise at equilibrium in terms of two shot-noise contributions associated with the thermal current $I_{\mathrm{Th}} = GKT/q$ oppositely injected from the contacts. Indeed, the use of a thermal voltage KT/q implies $S_{\mathrm{Ith}}^{\mathrm{Sh}}(0) = 2GKT$ and the fundamental property (ii) is no longer satisfied because GKT does not depend on the discreteness of the charge. We concentrate on shot-noise suppression in the next section.

3. Shot-noise Suppression

Shot noise and its suppression was considered for the first time in ballistic systems, such as vacuum tubes, following the seminal work of Schottky (1918), and was well understood in terms of the Poissonian statistics of different current pulses. Within this model, shot noise has been successively investigated also in other vacuum tubes (Thompson *et al.* 1940*a*, 1940*b*) and in several nonuniform devices such as Schottky diodes, p–n junctions, tunnel diodes, etc. (van der Ziel 1986).

Contrary to ballistic systems, in macroscopic structures, where inelastic scattering mechanisms with phonons, impurities and other carriers determine the transport properties, shot noise is not usually detected and noise levels close to the thermal value are typically measured (in the frequency range beyond $1/f$ and generation-recombination contributions) (Shimizu and Ueda 1992; Shimizu and Sakaki 1992; Büttiker 1995; Gonzalez *et al.* 1998*a*; Reklaitis and Reggiani 1997*a*, 1997*b*, 1999).

With the recent advent of mesoscopic devices, shot noise has received renewed attention. We remark that, with the term *mesoscopic* here, we generally refer to both classical (Galperin and Kozub 1991*a*, 1991*b*) and quantum structures in which the common feature is that the length of the active region is much smaller than that of the energy relaxation, usually called the phase-breaking length in the quantum case. In particular, being a signature of correlations among particles, the phenomenon of suppression has emerged as a subject of relevant interest in the wider field of correlated systems.

Among the mesoscopic devices exhibiting shot-noise suppression we recall: resonant and non-resonant tunneling diodes (Li *et al.* 1990*a*; Chen and Ting 1991; Davies *et al.* 1992; Liu *et al.* 1995; de Jong and Beenakker 1995; Iannaccone and Pellegrini 1997; Yan *et al.* 1997); the vacuum tunneling probe (Yurke and Kochanski 1990); small-size conductors (e.g. quantum point contacts, quantum and classical wires, metallic conductors, etc.—see Li *et al.* 1990*a*, 1990*b*; Liefrink *et al.* 1994; Reznikov *et al.* 1995; Kumar *et al.* 1996; Steinbach *et al.* 1996; Schoelkopf *et al.* 1997); and quantum beam-splitter structures (Liu *et al.* 1998).

Among the mechanisms responsible for shot-noise suppression (Landauer 1996, 1999) we mention: the long-range Coulomb interaction (space-charge) (van der Ziel 1954; Gonzalez *et al.* 1997*a*, 1997*b*) and screening (Naveh *et al.* 1997); the short-range Coulomb interaction (carrier–carrier interaction) (Hung and Wu 1993; Kozub and Rudin 1995*a*, 1995*b*; Nagaev 1995*a*, 1995*b*); the Pauli principle (Liu *et al.* 1998; Büttiker 1990; Martin and Landauer 1992; Altshuler *et al.* 1994; Liu *et al.* 1997); tunnelling processes within different transmission regimes (e.g. partition, coherent, sequential, etc.—see van der Ziel 1954; Dorokhov 1984; Imry 1986; Lesovik 1989; Yurke and Kochansnki 1990; Li *et al.* 1990*a*; van de Roer *et al.* 1991; Chen and Ting 1991, 1992; Beenakker and Büttiker 1992; Davies *et al.* 1992; Hung and Wu 1993; Hershfield *et al.* 1993; Hanke *et al.* 1993; Liu and Yamamoto 1994; Nazarov 1994; Sheng and Chua 1994; Liu *et al.* 1995; de Jong and Beenakker 1995; Birk and Schönenberg 1995; Jahan and Anwar 1995; Reznikov *et al.* 1995; Iannaccone and Pellegrini 1995, 1997; Kumar *et al.* 1996; Yan *et al.* 1997; Lund and Galperin 1997; Schep and Bauer 1997; Reklaitis and Reggiani 1997*a*, 1997*b*, 1999; Liu *et al.* 1998); and fractional charge (de Picciotto *et al.* 1997; Saminadayar *et al.* 1997).

Noticeably, most of the predictions concerning shot-noise suppression have been experimentally confirmed (Li *et al.* 1990*a*, 1990*b*; Liefrink *et al.* 1994; Liu *et al.* 1995, 1998; Reznikov *et al.* 1995; Kumar *et al.* 1996; Steinbach *et al.* 1996; Yan *et al.* 1997; Schoelkopf *et al.* 1997).

A great part of the theoretical work carried out so far considers degenerate conductors (often at zero temperature to avoid thermal noise), where the Pauli exclusion principle plays a major role. In contrast, the long-range Coulomb interaction among carriers and the effect of energy dissipation has received less attention. Accordingly, the main objective of this review is to provide a systematic analysis of shot-noise suppression in *nondegenerate* structures with the inclusion of Coulomb correlation and/or energy dissipation. Here two objectives are of main concern: (i) the determination of the suppression value when the transport regime is controlled by diffusion or tunneling, and (ii) an understanding of the progressive disappearance of shot noise when passing from the mesoscopic elastic regime (analogous to the coherent regime in the quantum case) to the macroscopic inelastic regime of conduction.

Our approach differs from those typically used to analyse shot-noise in quantum mesoscopic systems. Present calculations are based on an ensemble MC simulation self-consistently coupled with a Poisson solver (PS, where the scattering mechanisms and the fluctuations of the self-consistent potential are naturally accounted for at a kinetic level. In addition, the approach can analyse increasing applied voltages U, ranging from conditions near thermal equilibrium (i.e. $qU/KT \ll 1$) to conditions very far from equilibrium (i.e. $qU/KT \gg 1$),

without the difficulties that other methods meet (Green and Das 1998). These latter conditions are those necessary for shot noise to be dominant with respect to thermal noise.

4. Theoretical Model

The physical system of interest consists of a semiconductor structure sandwiched between two doped (but nondegenerate) contacts acting as ideal reservoirs, i.e. completely absorbing and thermalising, as sketched in Fig. 2, where n_c and N_D are the doping of the contacts and structure respectively. The structure is assumed to have a transversal size sufficiently thick to allow a 1D electrostatic treatment in the x direction and to neglect the effects of boundaries in the y and z directions. The structure will be specialised according to the transport regime analysed, i.e. ballistic/diffusive or tunneling controlled. The contacts are assumed to have no voltage drop inside and to remain always at thermal equilibrium. Accordingly, when a voltage is applied to the structure, all the potential drop takes place inside the active region, between the positions $x = 0$ and $x = L$. The time and energy statistics of the injecting contacts is detailed in the next section.

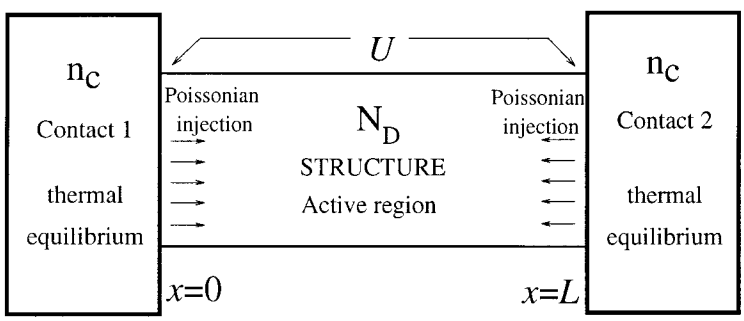

Fig. 2. Schematic drawing of the structure under investigation which includes the active region of the structure and the ideal contacts.

(4a) Contact Models

The modeling of carrier injection from the contacts can be crucial for the noise behaviour in mesoscopic devices, especially in the case of ballistic transport (Gonzalez *et al.* 1998*b*). To provide a complete model for the contacts and thus define the related sources of randomness in the carrier flux, we have to specify the velocity distribution of the injected carriers $f_{inj}(\mathbf{v})$, the injection rate Γ and its statistical properties. Here we have denoted $\mathbf{v} \equiv (v_x, v_y, v_z)$.

Let us consider the process of electron injection from contact 1 into the active region at $x = 0$ (see Fig. 2). According to the equilibrium conditions of the contacts, the injected carriers follow a Maxwellian distribution weighted by the velocity component v_x normal to the surface of the contact:

$$f_{\rm inj}(\mathbf{v}) = v_x f_{\rm MB}(\mathbf{v}), \quad v_x > 0\,, \tag{9}$$

where $f_{\rm MB}(\mathbf{v})$ is the Maxwell–Boltzmann distribution at the lattice temperature. The injection rate Γ, i.e. the number of carriers per unit time which enter the sample, is given by

$$\Gamma = n_c \bar{v}_+ S \,, \tag{10}$$

where S is the cross-sectional area of the device, and

$$\bar{v}_+ = \int_0^\infty \int_{-\infty}^\infty \int_{-\infty}^\infty f_{\rm inj}(\mathbf{v}) dv_x dv_y dv_z = \sqrt{\frac{KT}{2\pi m}} \,, \tag{11}$$

with m the carrier effective mass. The injection rate is taken to be independent of the applied voltage. Thus, the boundary injecting condition at the contacts is described through the constant injection rate Γ. The maximum current that a contact can provide in the ballistic limit is the saturation current $I_S = q\Gamma$.

According to the nondegenerate distribution of carriers, the random injection at the contacts is taken to follow Poissonian statistics. Thus, the time between the injection of two consecutive electrons, $t_{\rm inj}$, is generated with a probability per unit time given by

$$P(t_{\rm inj}) = \Gamma \exp(-\Gamma t_{\rm inj}) \,. \tag{12}$$

In the simulation we make use of equation (12) to generate $t_{\rm inj}$ which, following the MC technique, is given by $t_{\rm inj} = -(1/\Gamma)\ln(r)$, where r is a random number uniformly distributed between 0 and 1. Electrons are injected at $x = 0$ and $x = L$ into the active region of the structure according to the above stochastic rate. When a carrier exits through any of the contacts it is canceled from the simulation statistics, which accounts only for carriers that are inside the active region at the given time t. Thus, the instantaneous number of carriers in the sample $N(t)$ is a stochastic quantity which fluctuates in time due to the random injection/extraction from the contacts, and we can evaluate both the time-averaged value $\bar{N}$ and its fluctuations $\delta N(t) = N(t) - \bar{N}$.

Unless otherwise indicated, calculations make use of the above contact model, which appears to be physically plausible under nondegenerate conditions. However, to analyse the influence of the contact injecting statistics on the noise behaviour, alternative models are also used. In particular, for the injected carriers we consider: (i) a fixed velocity instead of Maxwellian distribution and (ii) uniform-in-time instead of Poissonian injection. In case (i) we consider the same injection rate Γ as in the basic model, but all carriers are injected with an identical x-velocity $v_x = \sqrt{\pi KT/2m}$, which corresponds to the average velocity of the injected electrons when they follow a Maxwellian distribution. In case (ii) carriers are injected into the active region equally spaced in time at intervals of $1/\Gamma$. Thus, the time between the injection of two consecutive electrons, $t_{\rm inj}$, is generated with a probability per unit time given by

$$P(t_{\rm inj}) = \delta(t - \Gamma^{-1}) \,. \tag{13}$$

(4b) Kinetic Approach

The kinetic approach makes use of an ensemble MC simulation 3D in momentum space coupled with a 1D PS (equivalent to a Boltzmann–Langevin approach). Electrons in the active region are considered as semiclassical particles, interacting

with the lattice. Elastic and inelastic scattering are considered. Electron tunneling across barriers is treated as an independent sequential process. Elastic tunneling probabilities for the triangular and trapezoidal potential are obtained from analytical solutions of the appropriate Schrödinger equation, as already used to study hot-carrier instabilities in similar structures (Reklaitis 1996*a*) and reported with details by Moglestue (1993), Reklaitis (1996*b*) and Reklaitis and Reggiani (1999).

According to the Ramo–Shockley theorem (Ramo 1939; Shockley 1938) and its generalisation (Pellegrini 1986, 1993*a*, 1993*b*), each electron moving inside the structure with an instantaneous velocity $v_i(t)$ along the field direction induces the instantaneous current $ev_i(t)/L$ in the external circuit, where L is the sample length. Therefore the fluctuating current in the external circuit is evaluated as

$$I(t) = \frac{q}{L} \sum_{i=1}^{N(t)} v_i(t) \,. \tag{14}$$

From a knowledge of the instantaneous current, the autocorrelation function of current fluctuations is calculated in the usual way (Varani *et al.* 1994) and the associated spectral density is obtained by Fourier transforming the current autocorrelation function. An uncertainty of 10% and 20% in the worst cases can be associated with numerical results pertaining to correlation functions and spectral densities, respectively.

5. Results

(5a) Nondegenerate Homojunction System

In the case of a nondegenerate homojunction system the structure in Fig. 2 consists of a lightly doped active region of a semiconductor sample sandwiched between two heavily doped contacts (of the same semiconductor) which act as thermal reservoirs and inject carriers into the active region. The doping of the contacts n_c is taken to be much higher than that of the active region N_D. The carrier density at the contacts corresponds to their doping concentration; all impurities are assumed to be ionised at the temperature $T = 300$ K considered here.

Typically, a 3D momentum space is considered. However, to analyse the influence of dimensionality on the noise suppression, a 2D and 1D momentum space is also considered in some specific cases. *Static* (i.e. a stationary electric field profile which is time independent) and *dynamic* PS schemes are used to analyse the importance of Coulomb correlations. The details of the MC modeling can be found in Gonzalez *et al.* (1997*a*, 1997*b*).

For the calculations we have used the following set of parameters: a carrier effective mass $m = 0{\cdot}25m_0$ (m_0 being the free electron mass), a dielectric constant $\varepsilon = 11{\cdot}7\varepsilon_0$ (ε_0 being the vacuum permittivity), $L = 2000$ Å, n_c ranging between 10^{13} and 10^{18} cm^{-3}, and $N_D = 10^{11}$ cm^{-3}. The injection rate at the contacts, Γ, is proportional to n_c and determines the level of space charge inside the active region, which is characterised by the dimensionless parameter λ, defined as (Gonzalez *et al.* 1997*b*, 1998*b*)

$$\lambda = \frac{L}{L_{Dc}} \,, \tag{15}$$

where $L_{Dc} = \sqrt{\varepsilon KT/q^2 n_c}$ is the Debye length corresponding to the carrier concentration at the contacts. In present calculations λ takes the minimum value of $0{\cdot}15$ ($n_c = 10^{13}$ cm^{-3}), for which the effects of Coulomb repulsion between electrons are practically negligible, and the maximum values of $30{\cdot}9$ ($n_c = 4 \times 10^{17}$ cm^{-3}) and $48{\cdot}8$ ($n_c = 10^{18}$ cm^{-3}), for which quite significant electrostatic screening takes place.

Scattering mechanisms are introduced in the simulation in a simple way by making use of an energy independent relaxation time τ. We consider separately elastic and inelastic (completely thermalising) interactions, both taken to be isotropic (Gonzalez *et al.* 1998*a*). While L remains constant, the value of τ is appropriately varied from 10 ps to 1 fs to continuously cover from ballistic to diffusive transport regimes. The transition between these regimes is characterised by the ratio between the carrier mean free path ℓ, defined as $\ell = 2\bar{v}_+\tau$, and the sample length L. Typical values of the time step and number of meshes in real space used for the PS are 2 fs and 100, respectively, except for the cases when $\tau < 5$ fs for which the time step is taken to be $0{\cdot}2$ fs. As a test of numerical reliability we have checked that by reducing the time step or by increasing the number of meshes the results remain the same. The average number of simulated particles in the active region ranges between 50 and 2000 depending on contact doping, transport regime, and applied voltage. The suppression factor is then evaluated as $\gamma = S_I(0)/2qI$. To distinguish between the results obtained from the static and dynamic PS, we denote the corresponding current spectral densities as S_I^s and S_I^d respectively.

The structures considered contain space charge in the active region, and the total charge neutrality is implicitly guaranteed by the much higher doping of the contacts with respect to that of the active region. In other words, the external circuit acts as a large grounding capacitor, thus ensuring charge neutrality in the whole system (Nagaev 1998*a*, 1998*b*). However, the effect of possible charge fluctuations at the contacts is not included in the calculation of the current. In any case, these effects are expected to appear at high frequencies (comparable with those of the plasma), while we are mostly interested in the low-frequency region of the noise spectrum.

Current–voltage (ballistic and diffusive). Fig. 3 reports the calculated current–voltage ($I-U$) characteristics of the structure shown in Fig. 2 for the (*a*) ballistic and (*b*) diffusive regimes. In the ballistic regime, the $I-U$ characteristics exhibit an almost linear behaviour before saturating to the maximum current the contact can supply I_S. At increasing space-charge effects, the potential minimum near the cathode increases thus limiting the number of carriers which reach the anode. Accordingly, the linear behaviour extends at higher voltages until the minimum disappears and the current saturates.

In the diffusive regime, because of scattering the current remains substantially lower than the saturation value in the whole voltage range analysed here. Furthermore, a slight super-ohmic behaviour is evidenced as expected by space-charge-limited current conditions (Lampert and Mark 1970). In the wide range of voltages reported in Fig. 3*b*, the $I-U$ curve exhibits a super-linear behaviour which is related to the importance of space-charge effects and the increase of the carrier number inside the active region with the applied voltage for $qU \gtrsim KT$. For the highest applied voltages it is found that $I \propto U^r$, where the power r is

a function of λ. In particular, $r = 1{\cdot}7$ for $\lambda = 30{\cdot}9$ and $r = 1{\cdot}8$ for $\lambda = 48{\cdot}8$. At low voltages, the determination of $S_I(0)$ can be carried out without major difficulties; however, the lowest value reported for the current corresponds to $I/I_S = 10^{-4}$. Indeed, below this value the statistical resolution of the simulation is no longer sufficient and the values of the current become unreliable. For $qU < KT$ we expect that the $I - U$ characteristic of the structures becomes linear because of the presence of two injecting contacts.

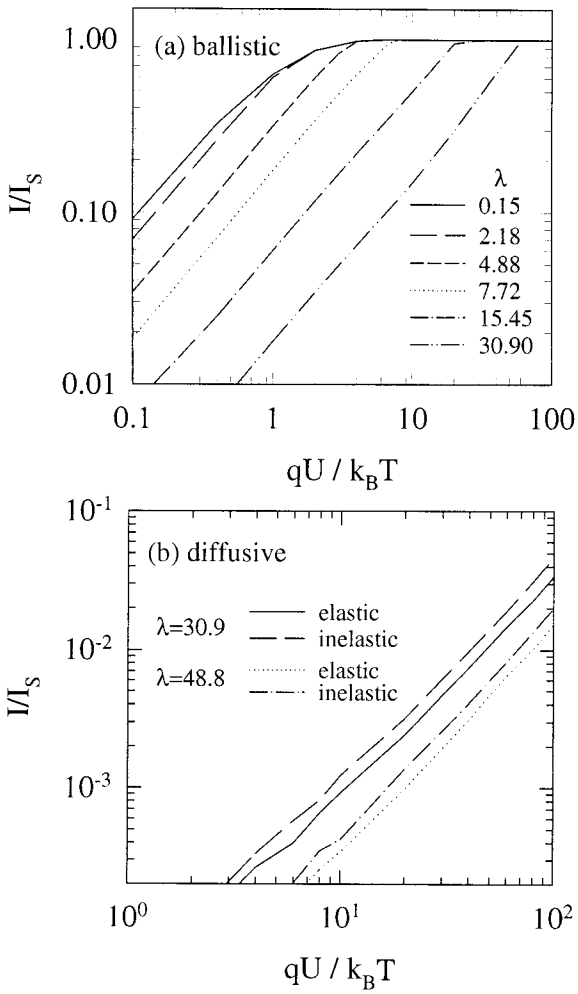

Fig. 3. Current–voltage characteristics of the homogeneous structure for the (*a*) ballistic and (*b*) diffusive regimes. The current is normalised to the saturation value and the voltage to the thermal value.

The main results concerning fluctuations are discussed in the next subsections, which are organised as follows. The first two pertain to a 3D momentum space, while the next is devoted to 2D and 1D momentum spaces. Most of the reported results refer to high values of the space-charge parameter λ (typically $\lambda = 30{\cdot}9$), which implies the presence of significant effects related to long-range Coulomb

interaction in the active region of the structures. In particular, a significant inhomogeneity in the charge distribution is present, as shown by Gonzalez *et al.* (1998*b*) in the ballistic case. We recall that elastic and inelastic scattering are considered separately in the simulations. In no case are both types of scattering taken into account simultaneously.

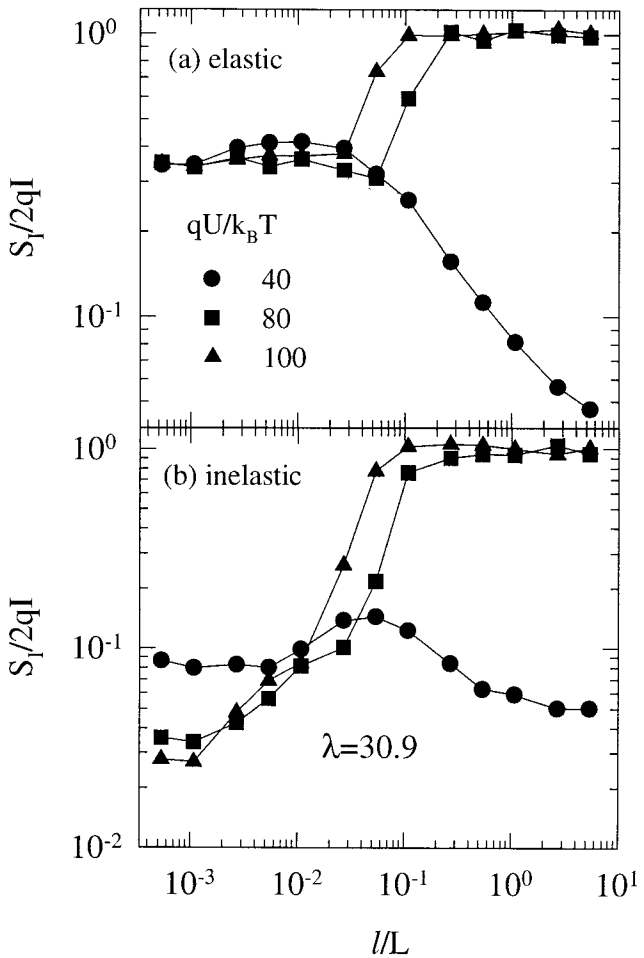

Fig. 4. Shot-noise suppression factor versus ballistic parameter ℓ/L for the cases of (*a*) elastic and (*b*) inelastic scattering at different applied voltages. Calculations are performed by using the dynamic PS scheme with $\lambda = 30{\cdot}9$.

Transition ballistic–diffusive regimes. The behaviour of noise in the crossover from ballistic to diffusive transport regimes is analysed under far-from-equilibrium conditions ($U \gg KT/q$), since these are necessary for the manifestation of shot noise. We consider the dynamic PS scheme. Fig. 4 reports γ as a function of ℓ/L for several values of the applied voltage in the (*a*) elastic and (*b*) inelastic cases respectively. In the perfect ballistic regime the two distinct values of γ found refer to the presence or absence of the potential barrier related to space

charge (Gonzalez *et al.* 1998*b*). For $U = 40\ KT/q$ the barrier is still present and the suppression is important. For $U = 80$ and $100\ KT/q$ the barrier has already disappeared; accordingly the current saturates and the suppression factor takes on the full shot-noise value. When the diffusive regime is achieved, in the elastic case γ attains a constant value at further decreasing values of ℓ/L, and takes the same value of about $\frac{1}{3}$ independently of the applied voltage. On the contrary, in the inelastic case the higher the applied voltage the lower the value which γ is found to take. Remarkably, the value of ℓ/L at which γ starts decreasing when the ballistic regime is abandoned is the same in the elastic and inelastic cases for a given applied voltage ($\ell/L \approx 0{\cdot}3$ and $0{\cdot}1$ for 80 and $100\ KT/q$ respectively). However, when the diffusive regime is approached, a lower value of ℓ/L must be reached in the inelastic case with respect to the elastic one for γ to take a constant value. This behaviour can be explained in terms of the different elastic and inelastic scattering intensity required by the electron system to achieve a significant equipartition of energy into the three directions of momentum space (Gonzalez *et al.* 1999).

To analyse the role played by the modeling of the contact injection on the suppression of noise, Fig. 5 reports γ as a function of ℓ/L calculated using four different contact models for the (*a*) elastic and (*b*) inelastic cases respectively. They combine Poissonian/uniform injecting statistics and a Maxwellian/fixed-velocity distribution of the injected carriers. The Poissonian–Maxwellian injection is the basic one used in calculations. In the perfect ballistic regime, when carrier transport is deterministic, γ crucially depends on the injection model. Thus, in the case of the uniform fixed-velocity model, when the injection introduces no extra noise in the current flux, γ is found to decrease linearly with an increase of ℓ/L. The noise does not vanish completely since, unless $\ell/L \to \infty$, there is always some probability of undergoing a scattering mechanism. In this limit, when the noise is produced just by a few scattering events, it is clearly observed that elastic interactions lead to more important current fluctuations than inelastic mechanisms. By approaching the perfect diffusive regime the suppression factor is found to be independent of the model used. We conclude that *the noise in the diffusive regime (and particularly the* $\frac{1}{3}$ *suppression value obtained in the elastic diffusive case) is independent of the carrier injecting statistics*, and it is only determined by the joint action of scattering mechanisms and Coulomb correlations.

Diffusive regime. In this subsection we consider scattering times short enough to ensure a diffusive transport regime ($\ell/L \lesssim 3 \times 10^{-3}$). In this regime the noise behaviour is closely related to the breadth of the velocity distribution (Landauer 1993; Nagaev 1995*a*). Fig. 6 shows $S_I(0)/2qI$ as a function of the applied voltage normalised to the thermal value for two values of the space charge shown in parts (*a*) and (*b*). To emphasise the shot-noise dependence on the discreteness of charge, in Fig. 6*a* we show also the results of simulations performed for the elastic case by scaling $q \to q/2$, $m \to m/2$, $n_c \to 4n_c$ and $S \to S/2$. This scaling preserves the values of the low-field conductance and λ (same space charge conditions) considered in Fig. 6*a*. The two elastic simulations performed with the unit and scaled value of the charge practically coincide in the thermal-Nyquist limit. On the contrary, they show shot-noise suppression factors of about $\frac{1}{3}$ and $\frac{1}{6}$, respectively, in the high-voltage limit, in accordance with the

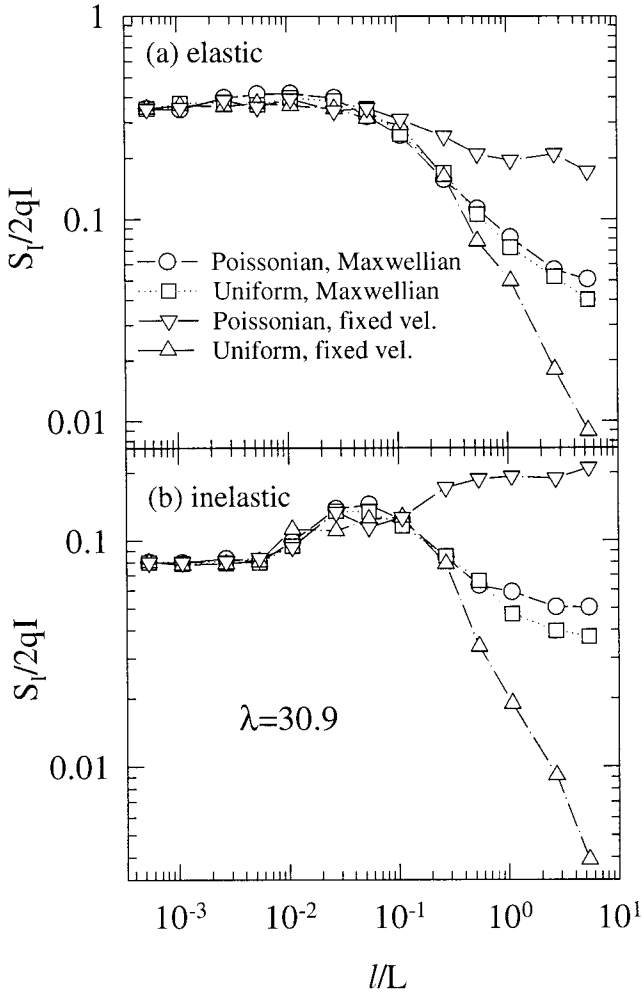

Fig. 5. Shot-noise suppression factor versus the ballistic parameter ℓ/L for an applied bias of $U = 40KT/q$ calculated with different contact models. Calculations refer to the dynamic PS scheme with $\lambda = 30{\cdot}9$ and consider (a) elastic and (b) inelastic scattering.

scaling of the charge. For both charge values, a smooth cross-over between the thermal-Nyquist and shot-noise regime takes place. From Fig. 6 it is observed that the the behaviour of γ is quite similar for both values of λ. By comparing in each part the results corresponding to elastic and inelastic scattering we find that, near thermal equilibrium conditions ($qU < KT$), both cases exhibit the same value which satisfies the Nyquist relation. On the contrary, at high voltages ($qU/KT \gtrsim 10$) the elastic case reaches the $\frac{1}{3}$ limiting value, while the inelastic case decreases systematically (Gonzalez *et al.* 1998*a*).

The MC results in the inelastic case $S_I^{\text{inel}}(0)$ are closely fitted by the expression

$$S_I^{\text{inel}}(0) = 4KTG_0\frac{\langle N\rangle}{\langle N\rangle_0}\,, \tag{16}$$

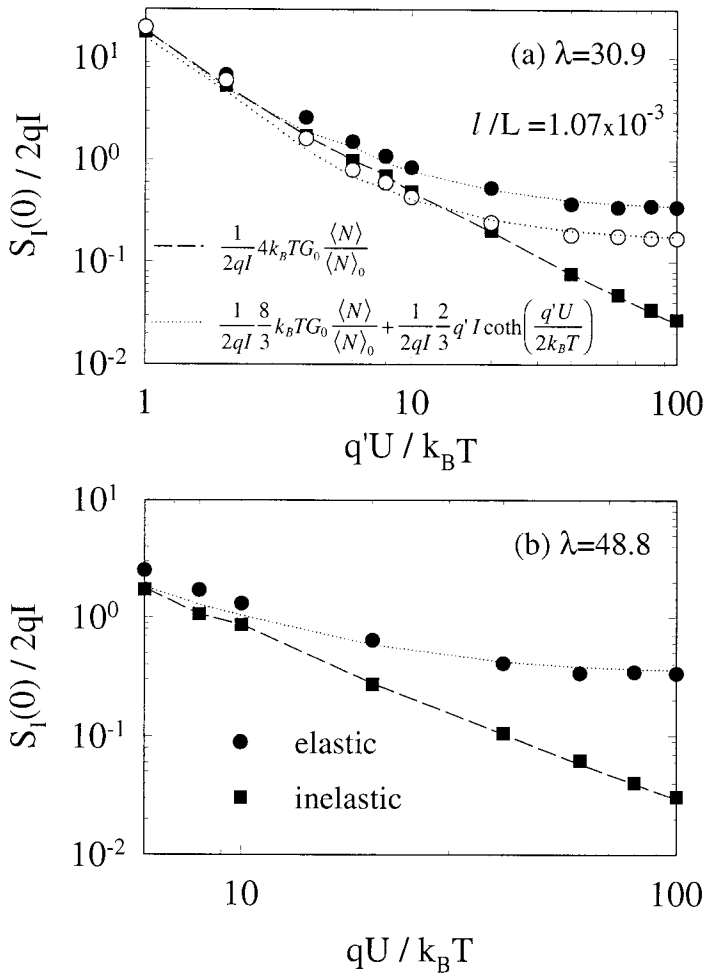

Fig. 6. Shot-noise suppression factor versus applied voltage for $\ell/L = 1{\cdot}07\times10^{-3}$. Calculations refer to the dynamic PS scheme considering elastic and inelastic scattering with (*a*) $\lambda = 30{\cdot}9$ and (*b*) $\lambda = 48{\cdot}8$. In Fig. 6*a* open circles correspond to the elastic case with the scaled values $q \to q/2$, $m \to m/2$, $n_c \to 4n_c$ and $S \to S/2$; and q' stands for q and $q/2$ in the results corresponding to unit and scaled charge. The fittings of equations (16) and (18) are shown by the dashed and dotted lines respectively.

where

$$G_0 = \frac{q^2\langle N\rangle_0\tau}{mL^2} \tag{17}$$

is the conductance and $\langle N\rangle_0$ the average number of electrons inside the sample, both in the limit of vanishing bias. Thus, in the case of inelastic scattering the spectral density can be expressed analogously to that of thermal Nyquist noise modulated by the variation of carrier number at the given voltage, even in the presence of a high bias and a net current flowing through the structure. Equation (16) describes correctly the thermal noise of the present structure, since the

non-linearity of the $I-U$ characteristic is taken into account through the factor $\langle N\rangle/\langle N\rangle_0$, which depends on the applied voltage. We conclude that inelastic scattering strongly suppresses shot noise and makes the noise become macroscopic ($\gamma \ll 1$) (Gonzalez *et al.* 1998*a*). We remark that present findings prove also that the condition of inelastic scattering alone does not suffice to suppress shot noise; the presence of the fluctuating self-consistent electric field remaining a necessary condition (Büttiker 1995). Indeed, as a counter-proof we refer to the calculations performed with the static PS scheme, where no suppression has been detected (Gonzalez *et al.* 1998*a*). Therefore, as argued by Büttiker (1995), *it is the combination of both Coulomb interaction and inelastic scattering which leads to the suppression of shot noise*. In the elastic case, the values of $S_I^{\rm el}(0)$ are nicely reproduced by the following expression:

$$S_I^{\rm el}(0) = \tfrac{8}{3}KTG_0\frac{\langle N\rangle}{\langle N\rangle_0} + \tfrac{2}{3}q'I\coth\left(\frac{q'U}{2KT}\right), \tag{18}$$

with q' taking the full q or the reduced $q/2$ charge value. Equation (18) is quite similar to that obtained by Nagaev (1992) in a degenerate context, and describes the smooth crossover from thermal-Nyquist noise for $q'U \ll KT$ to $\frac{1}{3}$ or $\frac{1}{6}$ suppressed shot-noise for $q'U \gg KT$.

In contrast to other approaches (Beenakker and Büttiker 1992; Nagaev 1992; de Jong and Beenakker 1995; Liu *et al.* 1997), our results show that, *neither phase-coherence* (Sukhorukov and Loss 1998) *nor degenerate statistics are required for the occurrence of suppressed shot noise in diffusive conductors*, and purely classical physical processes can lead to the same $\frac{1}{3}$ factor (Landauer 1998, 1999).

To illustrate the physical origin of the $\frac{1}{3}$ value, Fig. 7 reports a typical spectrum of the suppression factor under elastic diffusive conditions for the static and dynamic PS schemes. Here the current spectrum is decomposed into velocity, number, and cross-correlation contributions (Reggiani *et al.* 1992; Gonzalez and Pardo 1993; Gonzalez *et al.* 1997*b*):

$$S_I(f) = S_V(f) + S_N(f) + S_{VN}(f), \tag{19}$$

with

$$S_V(f) = 2\int_{-\infty}^{\infty}\frac{q^2}{L^2}\langle N\rangle^2\langle\delta v(0)\delta v(t)\rangle e^{i2\pi ft}dt, \tag{20}$$

$$S_N(f) = 2\int_{-\infty}^{\infty}\frac{q^2}{L^2}\langle v\rangle^2\langle\delta N(0)\delta N(t)\rangle e^{i2\pi ft}dt, \tag{21}$$

$$S_{VN}(f) = 2\int_{-\infty}^{\infty}\frac{q^2}{L^2}\langle v\rangle\langle N\rangle[\langle\delta v(0)\delta N(t) + \delta N(0)\delta v(t)\rangle]e^{i2\pi ft}dt. \tag{22}$$

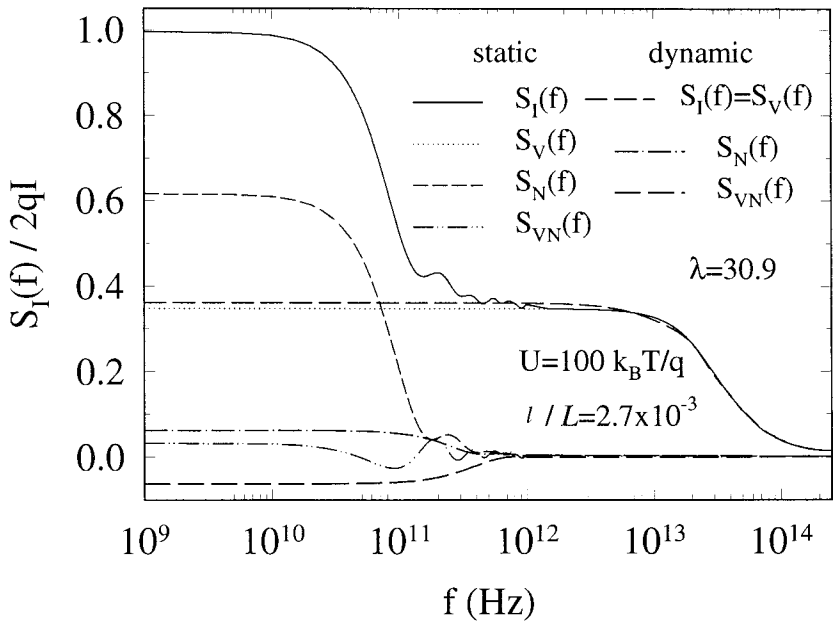

Fig. 7. Spectrum of the shot-noise suppression factor under the diffusive regime ($\ell/L = 2{\cdot}7 \times 10^{-3}$) calculated within static and dynamic PS schemes for the elastic case and an applied voltage of $U = 100\ KT/q$. Different contributions to the total spectrum are shown.

In the static PS scheme the spectrum clearly shows that the three terms contribute to $S_I(f)$, and two different time scales can be identified. The longest one is associated with the transit time of carriers through the active region $\tau_T \approx 5$ ps, and is evidenced in the terms $S_N^s(f)$ and $S_{VN}^s(f)$. The shortest one is related to the relaxation time of elastic scattering $\tau = 5$ fs, and is manifested in $S_V^s(f)$. Remarkably, the velocity contribution yields $\frac{1}{3}$ of the full shot-noise value, while the other two terms provide the remaining $\frac{2}{3}$. Thus, in the static PS scheme the full shot noise is recovered as sum of all three contributions. On the contrary, in the dynamic PS scheme $S_N^d(f)$ and $S_{VN}^d(f)$ are found to compensate each other and, as a result, $S_I^d(f)$ coincides with $S_V^d(f)$ in all the frequency range. Moreover, $S_N^d(f)$ takes values much smaller than $S_N^s(f)$. The characteristic time scale of $S_N^d(f)$ and $S_{VN}^d(f)$ differs from that found within the static PS scheme, which was related to the transit time τ_T. Now, in the dynamic case it is the dielectric relaxation time corresponding to the carrier concentration at the contacts $\tau_d = 0{\cdot}46$ ps which determines the cutoff of the contributions belonging to number fluctuations. In the frequency range between the transit and collision frequency values it is interesting to notice that both static and dynamic PS schemes yield $\gamma = \frac{1}{3}$, thus relating the suppression factor to velocity fluctuations only. However, at low frequencies only the dynamic scheme takes this value by virtue of Coulomb correlations, which are responsible for the reduction of $S_N^d(f)$ and the mutual compensation of $S_N^d(f)$ and $S_{VN}^d(f)$ contributions. It is remarkable that $S_V^s(f) = S_V^d(f)$ over all the frequency range, which implies that velocity fluctuations are not affected by the long-range Coulomb interaction, but only by scattering mechanisms. Coulomb repulsion affects only the contributions where carrier-number fluctuations are involved.

Dependence on momentum space dimensionality. The results reported so far refer to a 3D momentum space. In contrast to degenerate diffusive systems where, provided quasi-one dimensional conditions in real space are attained, noise suppression is independent of the number d of momentum space dimensions. An interesting feature of nondegenerate diffusive systems is that noise suppression can depend on d. For the inelastic case considered here no dependence on d has been found, since there is no influence of the velocity components transverse to the electric field direction on transport and noise properties of the structures. On the contrary, in the elastic case the suppression factor is found to depend significantly on d (Gonzalez *et al.* 1998*a*) since the transverse velocity components constitute a channel for energy redistribution which affects the transport properties of the structure. Therefore, below we focus our analysis on the elastic case. Accordingly, when $d = 2$ in the simulation the carrier velocity is randomised in two components after each scattering event, and when $d = 1$ the isotropic character of scattering is accomplished by inverting the carrier velocity with an average (back-scattering) probability $P_b = 0{\cdot}5$.

Fig. 8*a* reports γ as a function of ℓ/L for the 1D, 2D and 3D cases at high voltages ($U = 40KT/q$), calculated within the dynamic PS scheme. We notice that, when calculated within the static PS scheme, the results in the 1D and 2D cases do not exhibit any shot-noise suppression, like in the 3D case. For the highest values of ℓ/L, in all three cases γ approaches the asymptotic value corresponding to the ballistic limit ($\gamma = 0{\cdot}045$) (Gonzalez *et al.* 1997*b*), where the behaviour is practically independent of d. At a given value of ℓ/L, a higher deviation from the asymptotic ballistic value is observed for lower d. This is due to the fact that, on average, elastic interactions introduce higher fluctuations of the carrier x-velocity the lower the number of available momentum states after the scattering mechanism (in particular just two in the 1D case). For this same reason, the increasing presence of scattering as ℓ/L is reduced leads to higher values of the suppression factor, the lower the dimensionality. Remarkably, within numerical uncertainty, the limit value reached by γ in the perfect diffusive regime is found to be, respectively, $\frac{1}{3}$, $\frac{1}{2}$ and $0{\cdot}7$ for 3D, 2D and 1D. The appearance of the $\frac{1}{3}$ factor in the 1D MC simulation of Liu *et al.* (1997) does not contradict the present results because there it was due to the effect of the Pauli exclusion principle, while here the correlation between electrons comes from their Coulomb repulsion. Fig. 8*b* shows γ in the diffusive regime as a function of the applied voltage, providing evidence that these limit values are independent of the bias once $qU \gg KT$. The origin of the suppression is the same in all three cases: the joint action of Coulomb correlations and elastic scattering, which leads to the result $S_I(0) = S_V(0)$ (as shown in Fig. 7 in the 3D case), where $S_V(0)/2qI$ under the perfect diffusive regime is a function of the dimensionality of momentum space.

(5b) Tunneling Heterojunction System

In this section the physical systems under investigation are single and multiple barrier non-resonant diodes. Accordingly, the structure in Fig. 2 consists of GaAs/AlGaAs heterostructures sandwiched between appropriate emitting and collecting contacts. Contacts are considered to be ohmic, the voltage drop inside them being negligible, and to remain always at thermal equilibrium. If not

stated otherwise, electrons are emitted from the contacts according to a thermal equilibrium Maxwell–Boltzmann distribution at the temperature $T = 77$ K and with a Poissonian distribution in time.

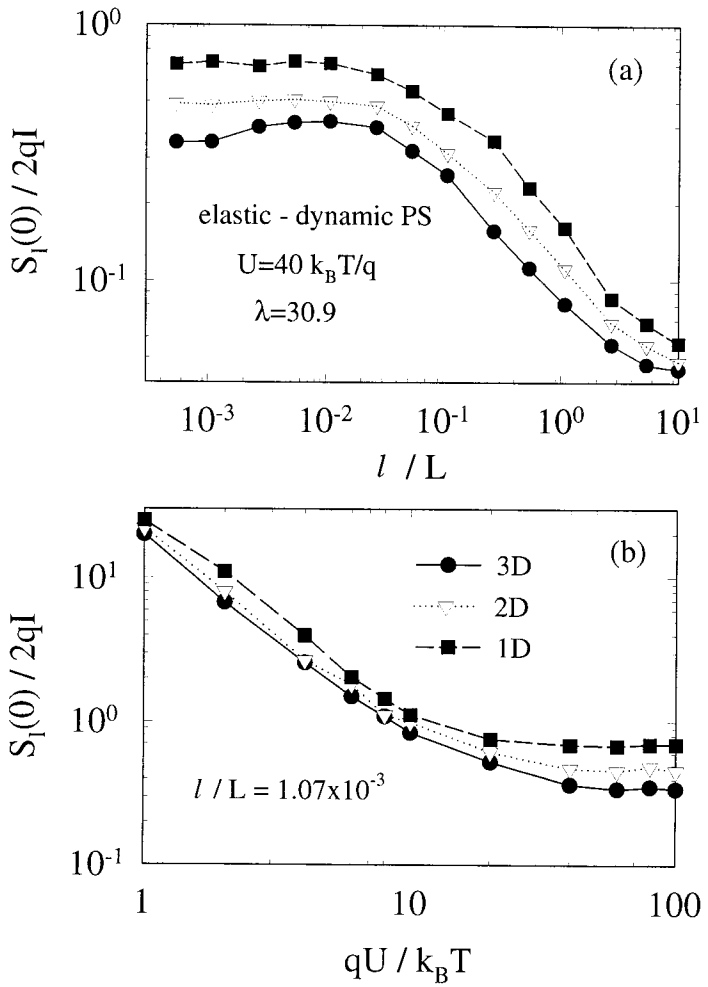

Fig. 8. Shot-noise suppression factor for the cases of 1, 2 and 3 dimensions of momentum space calculated within the dynamic PS scheme for elastic scattering as a function of: (*a*) the ballistic parameter ℓ/L with an applied voltage of $U = 40\ KT/q$ and (*b*) the applied bias U under diffusive regime ($\ell/L = 1{\cdot}07 \times 10^{-3}$).

The thicknesses of the GaAs layers are taken sufficiently large so that interference effects between AlGaAs barriers can be neglected. Electrons in the GaAs layers are then considered as semiclassical particles moving in the self-consistent electric field, interacting with phonons and ionised impurities, and their tunneling across a given barrier is treated as an independent sequential process occurring locally in space and time.

The analytical expressions for the energy dependence of the tunneling probabilities are obtained from analytical solutions of the appropriate Schrödinger equations

within the transfer matrix approach for triangular (Reklaitis 1996*a*) and trapezoidal (Reklaitis 1996*b*) potential barriers. They account for the discontinuity of effective masses at the hetero-interfaces. These probabilities are then used in MC simulations according to the energy of the impinging electron, trapezoidal for the low energy, and triangular for the high energy, respectively. The energy dependence of the tunneling probability is calculated for each electron impinging the barrier. The shapes of the potential barriers are updated each time step from the solution of the Poisson equation. The tunneling process is then treated in the MC simulation as a scattering event in what concerns the determination of the final state.

In the following we report the results of MC simulations on structures with increasing degrees of complexity.

Single barrier. The single barrier structure investigated here consists of three layers involving two GaAs layers and one $Al_{0\cdot25}Ga_{0\cdot75}As$ barrier. The structure is sandwiched between emitter and collector contacts. The length of the GaAs layer adjacent to the emitter is taken to be 500 Å, and that of the GaAs layer adjacent to the collector 800 Å. The length of the undoped $Al_{0\cdot25}Ga_{0\cdot75}$ As barrier is taken to be 40 Å. The GaAs layers adjacent to the emitter and the collector are doped with 5×10^{15} cm^{-3} donor concentration. The emitter and collector contacts are doped with 10^{17} cm^{-3} donor concentration. Fig. 9 shows the potential profile (solid line), and the distribution of electron kinetic energy (points) for a bias voltage of 0·5 V applied to the single barrier diode studied here in the presence of scattering mechanisms.

Fig. 10 reports the calculated $I-U$ characteristics of the diode shown in Fig. 9 for two cases, namely, when scattering is neglected (ballistic regime) and included (diffusive regime). In the ballistic regime the $I-U$ characteristic of the diode is determined by the tunneling probability averaged over the distribution function of electrons impinging on the barrier. The situation is more complex in the diffusive regime, especially when inelastic scattering by optical phonons becomes relevant. In this condition, the diode switches from a low conductance state to a high conductance state at $U \simeq 0\cdot9$ V (see Fig. 10). In both regimes, at the highest voltages the current saturates to a value corresponding to the maximum current the contact can supply, I_S, which in the present case corresponds to a current density of about 80 KA cm^{-2}. Fig. 11 shows the Fano factor versus voltage (to avoid thermal noise we consider the condition $qU \gg KT$) for the diode of Fig. 9 in the diffusive regime. Values of γ obtained from the calculated values of $S_I(0)$ and I (MC results) are compared with those calculated by the average partition expression (Davies *et al.* 1992; Reklaitis and Reggiani 1999):

$$\gamma = 1 - \frac{\langle D^2 \rangle}{\langle D \rangle}, \tag{23}$$

where $\langle D \rangle$ and $\langle D^2 \rangle$ are the tunneling probabilities and its square velocity-weighted averaged over the distribution function of the incident stream. Full shot noise is found at low bias voltages when the energy of electrons is much lower than that of the barrier and, in turn, the tunneling probability is much less than unity. At increasing voltages the electrons impinging the barrier become more energetic and shot noise is found to be suppressed. Here, the Fano factor directly

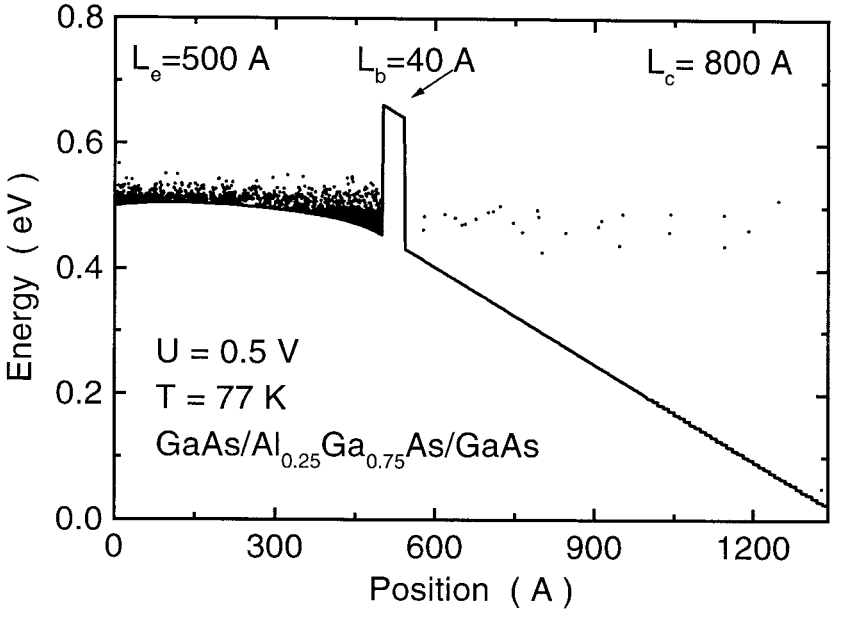

Fig. 9. Potential profile (solid line) and distribution of electron kinetic energy (points) for a voltage of 0·5 V applied to the single barrier diode studied here at $T = 77$ K.

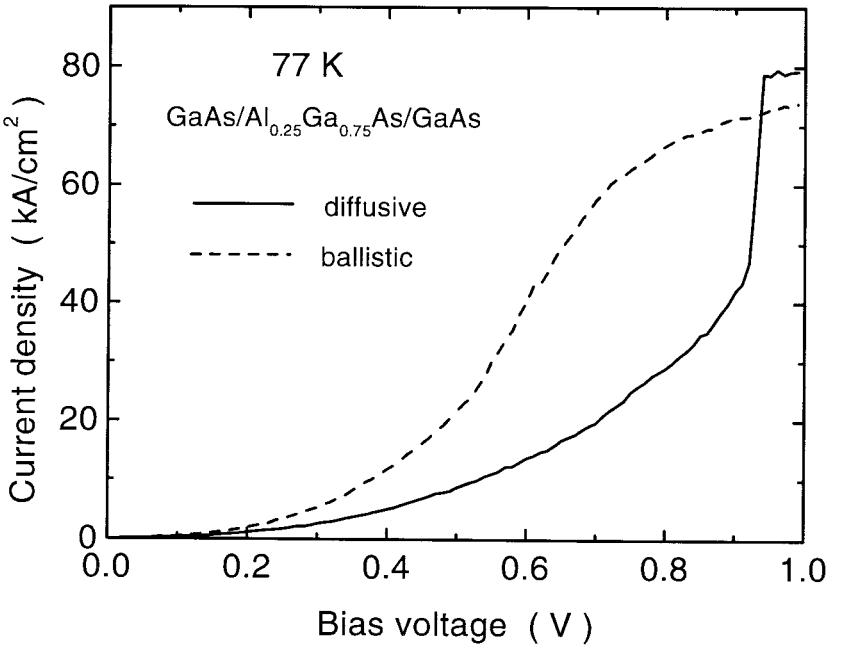

Fig. 10. Current–voltage characteristic of the diode in Fig. 9 for the ballistic (without scattering) and diffusive (with scattering) transport regimes.

obtained from MC exhibits a minimum value of about 0·86 at 0·5 V which is mostly attributed to the mechanism of suppression of independently transmitted electrons associated with optical phonon emission (Reklaitis and Reggiani 1999). Indeed, due to inelastic emission processes electrons have insufficient energy to come back to the emitter contact and remain confined in the region before the well. This confinement implies a nonuniformity of the electron flux incident on the barrier, since the temporal distribution of the electrons impinging the barrier depends on the number of tunneled electrons during a previous time moment. Suppression of shot noise is thus obtained as a consequence of this correlation.

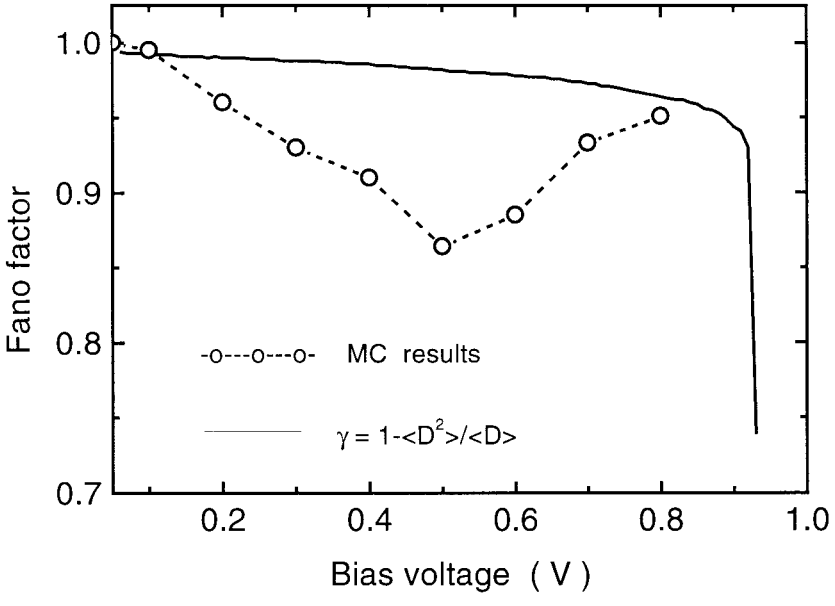

Fig. 11. Fano factor versus bias voltage obtained for the single barrier structure of Fig. 9 in the diffusive regime from direct MC calculations (open circles) and evaluated from the analytical partition relation (solid line).

It should be pointed out that the result is found to be essentially independent of the statistics used to inject electrons from the contacts. On the other hand, the Fano factor calculated by the partition expression remains practically equal to 1 up to voltages of about 0·8 V, as shown by the continuous curve in Fig. 11. At the highest applied voltages, the situation is the opposite because here the tunneling probability approaches unity. Accordingly, direct results are conditioned by the raised thermal fluctuations of hot electrons which are induced by phonon scattering, and the corresponding γ approaches unity (Gonzalez *et al.* 1998*a*). On the contrary, results calculated with the average partition expression of equation (23) drop quickly to zero. Anyway, the simple expression given by equation (23), being appropriate for a uniform injection of carriers impinging on a barrier and otherwise moving within a ballistic regime, is no longer justified at high voltages.

Double barrier. The double barrier structure investigated here consists of five layers involving three GaAs layers and two $Al_{0\cdot25}Ga_{0\cdot75}As$ barriers. The length

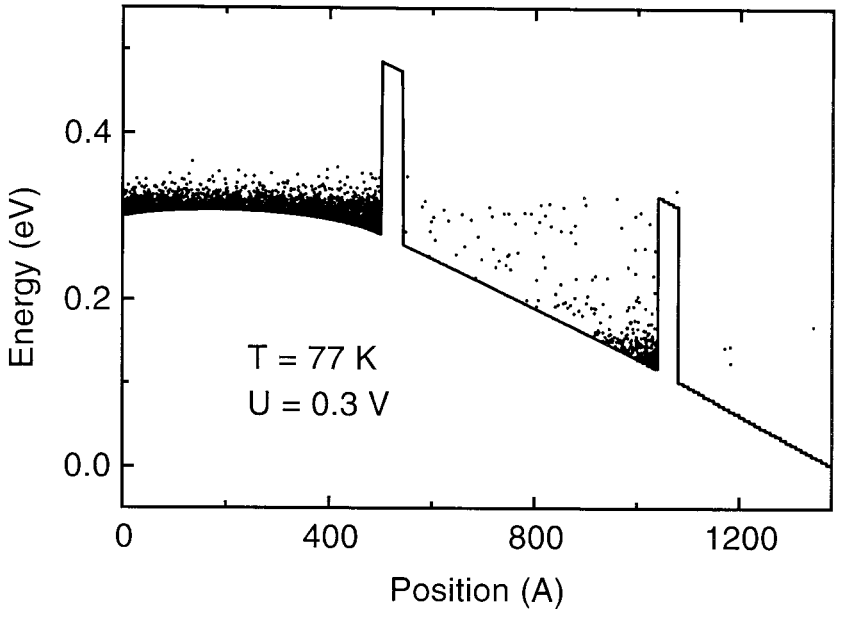

Fig. 12. Potential profile (solid line) and distribution of electron kinetic energy (points) for a voltage of 0·3 V applied to the double barrier diode studied here at $T = 77$ K.

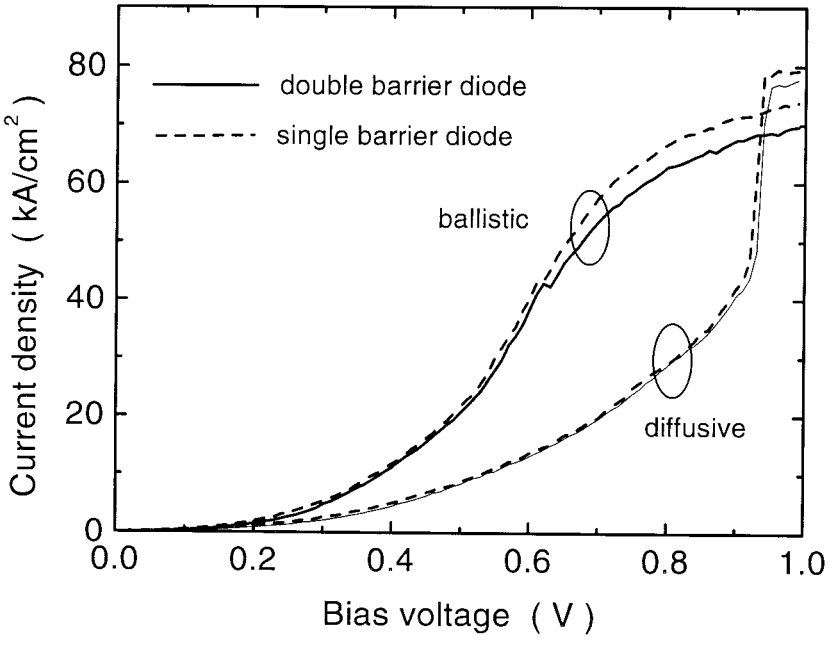

Fig. 13. Current–voltage characteristic of the diode in Fig. 12 for the ballistic (without scattering) and diffusive (with scattering) transport regimes. For comparison the characteristics of the single barrier diode are also shown.

of the GaAs layer adjacent to the emitter is taken to be 500 Å, that of the GaAs layer separated by the barriers 500 Å, and that of the GaAs layer adjacent to the collector 300 Å. The lengths of the undoped $Al_{0\cdot25}Ga_{0\cdot75}As$ barriers are taken to be 40 Å each. The GaAs layers adjacent to the emitter and the collector are doped with 5×10^{15} cm^{-3} donor concentration. The emitter and collector contacts are doped with 10^{17} cm^{-3} donor concentration. Fig. 12 shows the potential (solid line) and the distribution of electron kinetic energy (points) for an applied voltage of 0·3 V in the diffusive regime.

Fig. 13 reports the calculated $I-U$ characteristic of the structure shown in Fig. 12 for the ballistic and diffusive regimes. For comparison the same characteristics of the single barrier diode are also reported. The $I-U$ characteristics of the single and double barriers do not differ significantly from each other and both exhibit a superlinear behaviour before saturating (when the current reaches the contact injecting value). Indeed, the $I-U$ characteristic is controlled by the tunneling current across the barrier adjacent to the emitter in the range of bias voltage $U > KT/q$. The barrier adjacent to the collector has little effect on the current in this range of voltages because most electrons, after tunneling through the first barrier, are successfully tunneled across the second one, and do not come back to the emitter.

Fig. 14 reports the tunneling probabilities mentioned above as obtained from MC calculations in the presence of scattering. Here the subscripts 1 and 2 refer to the barrier label and the superscripts + and − to the case when an electron impinges on the barrier from the left and the right side respectively. The average values $\langle\rangle$ are over the corresponding distribution functions of impinging electrons. Note that these distributions are different for electrons impinging from the left and from the right. In the MC procedure the value of the total transmission probability $\langle D_1\rangle$ and $\langle D_2\rangle$ for each barrier is calculated by summing the $D^+(\mathbf{k})$ and $D^-(\mathbf{k})$ ($\mathbf{k}$ being the wave-vector of the impinging electron) contribution and then averaging the sum over the distribution function. Fig. 15 reports the Fano factor versus applied voltage of the double barrier of Fig. 12. Here the data refer to the diffusive regime as obtained directly from MC simulations together with that calculated in another context from a semiclassical theory by de Jong and Beenakker (1995) as

$$\gamma = \frac{\langle D_1^2\rangle(1-\langle D_2\rangle) + \langle D_2^2\rangle(1-\langle D_1\rangle)}{(\langle D_1\rangle + \langle D_2\rangle - \langle D_1\rangle\langle D_2\rangle)^2}\,, \tag{24}$$

where the angle bracket mean a velocity-weighted average over the distribution function of the incident stream across the emitter (1) and collector (2) barriers respectively. The curve by Chen and Ting (1991) in Fig. 15 corresponds to the simplified version of equation (24) when $\langle D_1\rangle, \langle D_2\rangle \ll 1$ are assumed.

In the range of low voltages we find that shot noise is significantly suppressed to a minimum level of $\gamma = 0\cdot58$ and thus essentially less than unity. At the highest voltages γ tends to unity. The calculations from equation (24) are found to agree satisfactorily with those obtained from the simulation (open circles) at the lowest voltages, while at increasing voltages they systematically overestimate the MC results. Accordingly, a value of γ close to 0·5 is obtained at the lowest voltage $U = 0\cdot2$ V when the tunneling probabilities across the emitter and

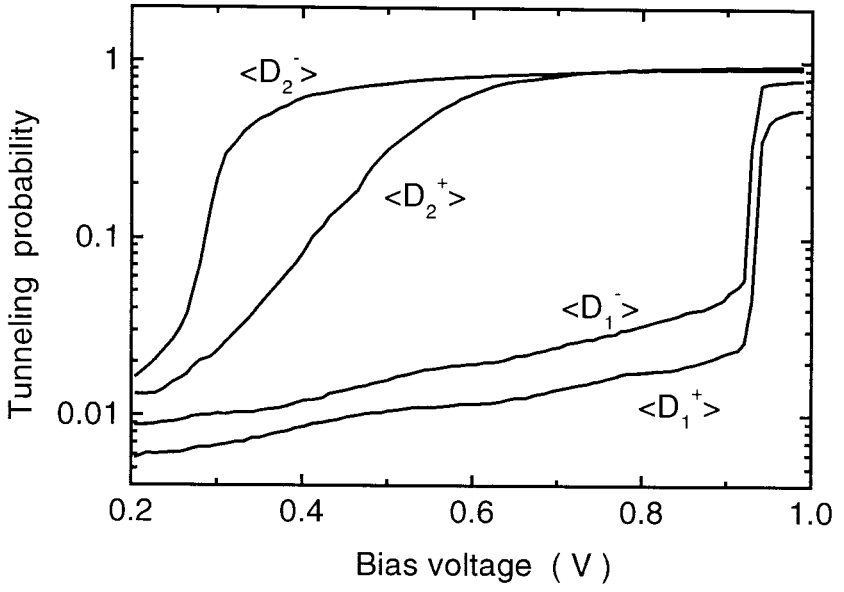

Fig. 14. Average tunneling probabilities of the double-barrier diode in Fig. 12 versus the applied voltage. Average values are taken over the corresponding distribution functions of electrons impinging on the left (+) and right (−) sides of each barrier.

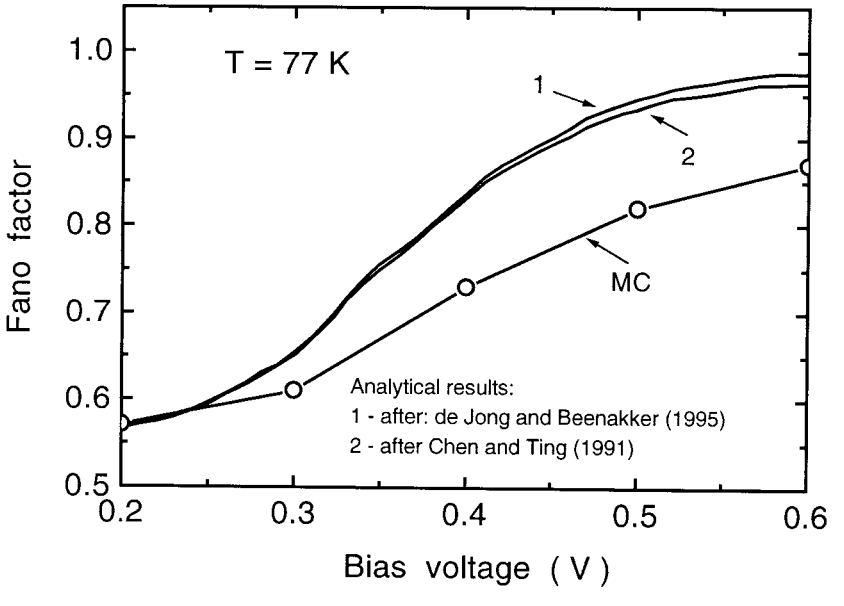

Fig. 15. Fano factor versus bias voltage obtained for the double barrier structure from direct MC calculations (open circles) and evaluated from the analytical relations (Chen and Ting 1991; de Jong and Beenakker 1995) (solid curves).

collector barriers are nearly equal and both much less than unity (see Fig. 14). At higher voltages, the barriers become asymmetric, i.e. $\langle D_1 \rangle \ll \langle D_2 \rangle \simeq 1$, and the values of γ increase towards unity. We notice that equation (24) has been obtained for a suppression mechanism associated with the Pauli principle and when elastic tunneling between the two barriers is considered. Thus, the overall agreement found with the present case, where the suppression mechanism is mostly attributed to inelastic scattering, remains an intriguing and not yet explained result. The repeated occurrence of a minimum value of $\gamma \simeq 0{\cdot}5$ for a double barrier structure when the tunneling probabilities are much smaller than unity leads us to believe that this must be more than a numerical coincidence (Macucci and Pellegrini 1995). We conjecture that the presence of inelastic scattering is analogous to the presence of a resonance inside the barriers in the sense that both destroy the otherwise uncorrelated motion of carriers between the two barriers, thus leading to shot-noise suppression when the tunneling probabilities are much smaller than one.

In order to check the influence on the shot noise of carrier injection statistics from the heavily doped contacts, we have also performed calculations considering a uniform model, instead of the Poissonian injection model. No difference has been observed between the results obtained with the two injection models.

The feedback between the fluctuating electron space charge in the GaAs well and the tunneling probabilities $\langle D_1 \rangle$ and $\langle D_2 \rangle$ can also influence the noise characteristics. In order to check this possible influence we have carried out MC simulations by using the self-consistent, but non-fluctuating, potential distribution. No difference has been detected for the low-frequency noise thus confirming the expectation that, for the chosen doping concentration, space-charge fluctuations play no role.

We conclude that the main contribution to the current noise is associated with tunneling processes and that equation (24), even if obtained under degenerate conditions and in the absence of scattering, is sufficiently adequate even under nondegenerate conditions and in the presence of scattering.

In the range of low voltages where shot noise is significantly suppressed to a level with $\gamma \simeq 0{\cdot}5$, existing theories (Chen and Ting 1991, 1992; Davies *et al.* 1992; de Jong and Beenakker 1995; de Jong 1996; Iannaccone and Pellegrini 1997) predict that such a suppression is basically due to correlations coming from the Pauli exclusion principle. Here, we have found that the shot-noise suppression can be explained within a simplified model which considers electron transmission from the first barrier, their oscillating motion in the well under the presence of inelastic scattering mechanisms which inhibit their return to the emitter, and their final tunneling across the second barrier with constant probability (Reklaitis and Reggiani 1999).

Extension to a multiple barrier. The features of shot-noise suppression are essentially changed when a third or more barrier structure is considered. Then the regulation of the electron motion due to the presence of inelastic scattering by optical-phonon emission can lead to a further suppression of shot noise. To this purpose, we have investigated the noise properties of GaAs/AlGaAs heterostructures which involve an increasing number of barriers up to four, which represents an upper limit of application for the present code. The unit cell of the multibarrier structures investigated here involves an undoped GaAs layer

followed by an undoped $Al_{0\cdot25}Ga_{0\cdot75}As$ barrier. The length of the GaAs layer is taken to be 500 Å, and that of the $Al_{0\cdot25}Ga_{0\cdot75}As$ barriers to be 40 Å. In each structure, an undoped GaAs layer of 300 Å length is sandwiched between the last barrier and the collector. The doping concentration of the contacts is taken at a low value of 10^{14} cm^{-3}.

The undoped heterostructures are taken to avoid the correlations which may be induced by long-range Coulomb interaction, thus being in the position to investigate the properties of the proposed model. Calculations for a realistic (from the experimental point of view) contact doping concentration of 10^{17} cm^{-3} are also carried out for the sake of comparison.

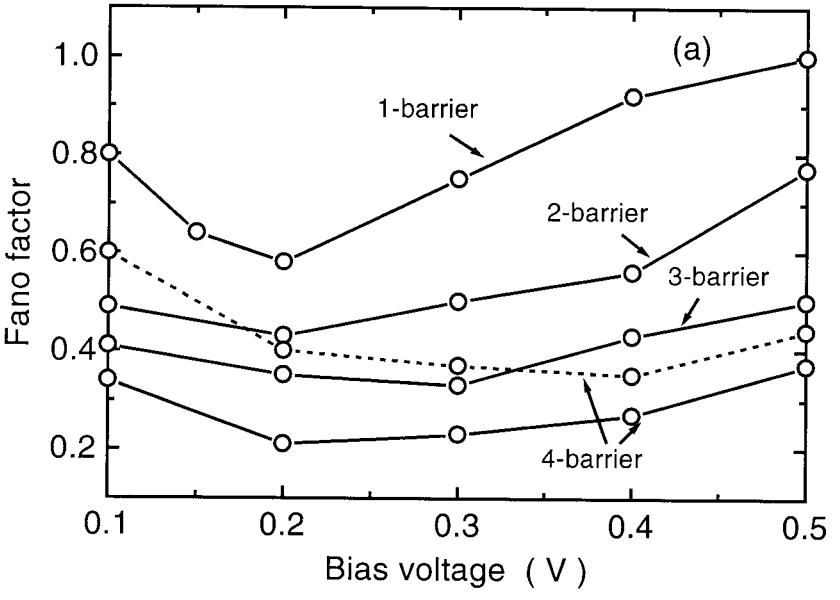

Fig. 16. Fano factor versus bias voltage for one, two, three and four barrier structures obtained from direct MC calculations. Solid lines report the results obtained for contact concentrations of 10^{14} cm^{-3}. The dashed line reports the results for the four-barrier structure with a contact doping concentration of 10^{17} cm^{-3}.

Results are reported in Fig. 16. By increasing the number of barriers, the Fano factor is found to reduce systematically, besides exhibiting a significant voltage dependence. The suppression factor in the structure consisting of four barriers and low-doping contacts is found to be essentially below the level of $\frac{1}{3}$ which is predicted by diffusive transport under elastic scattering conditions in degenerate (Beenakker and Büttiker 1992; Nagaev 1992; Altshuler *et al.* 1994; de Jong and Beenakker 1995; Liu *et al.* 1997; Blanter and Büttiker 1997) and nondegenerate (Gonzalez *et al.* 1998*a*) conductors (as shown in the previous results for the homojunction system). In particular, the minimum value of suppression is practically independent of voltage and follows approximately a $1/(N+1)$ behaviour, with N the number of barriers. This behaviour agrees with that expected for $(N+1)$ uncorrelated noise generators, as predicted by Landauer (1996; 1999) for a chain of thermionic diodes in series. The present mechanism, however, does not require the large number of electrons necessary

to realise an independent reservoir for each diode in the chain, thus offering a complementary model of suppression. For the sake of completeness, simulations of the four barrier structure with a contact doping concentration of 10^{17} cm^{-3} are also carried out. The corresponding results reported in Fig. 16 show that the Fano factor of that structure lies between those of the three- and four-barrier structures with lower contact doping. This result demonstrates that the presence of highly doped contacts, by simply implying an initial region with a nearly flat potential profile, would not change the essence of the results.

It should be pointed out that the $I-U$ characteristics of all the diodes with low-doped contacts are very close to each other. This behaviour is explained by the fact that the current in all diodes is controlled by the tunneling current across the barrier adjacent to the emitter in the range of bias voltage $\Delta U > KT/q$, ΔU being the potential drop in the GaAs layer adjacent to the emitter. As a consequence, the remaining barriers have a small effect on the *dc* current since most electrons, after tunneling through the first barrier and after subsequent phonon emission, are successfully tunneled across the remaining barriers, and do not come back to the emitter. Thus we obtain the interesting situation that in the intermediate range of voltages (0·1–0·5 V) the signal-to-noise ratio of the structures considered here can be significantly improved by increasing the number of barriers.

6. Conclusions

We have provided a microscopic analysis of shot-noise suppression in nondegenerate ballistic and diffusive semiconductor structures. To this purpose, the carrier dynamics in the active region of the structure under the dominant influence of (i) elastic or inelastic scattering and (ii) elastic tunneling processes has been simulated by using an ensemble Monte Carlo technique self-consistently coupled with a PS.

For the case of a homogeneous structure the essential role played by the long-range Coulomb interaction on the shot-noise suppression factor γ has been demonstrated, since no suppression is found in the absence of the self-consistent potential fluctuations. We have analysed shot-noise suppression in the region of crossover from ballistic to diffusive transport regimes. In the diffusive regime a value of γ independent of sample length is not achieved until a significant energy redistribution among momentum directions takes place. For high voltages $qU/KT \gg 1$ and long samples $\ell/L \ll 1$, in the elastic case shot noise is found to be suppressed to a value of $\frac{1}{3}$, while in the inelastic case we have found a stronger suppression the higher the applied voltage. Noticeably, in the perfect diffusive regime γ is found to be independent of carrier injecting statistics, which implies that in this regime the noise is just a property of the sample.

Our results show that neither phase coherence nor Fermi statistics are necessary for the appearance of the $\frac{1}{3}$ suppression factor in an elastic diffusive conductor. In our model, the appearance of this factor requires the simultaneous fulfillment of the following three conditions: $\ell/L \ll 1$, $\lambda \gg 1$ and $qU/KT \gg 1$. The first implies a perfect diffusive regime, the second strong space-charge effects, and the third very far-from-equilibrium conditions. Inelastic scattering is found to further contribute in suppressing shot noise, by reducing it to values close to thermal Nyquist noise under strong dissipative conditions. However, for this suppression

to take place the presence of the long-range Coulomb interaction is necessary.

The action of Coulomb repulsion in suppressing shot noise takes place through the reduction of the contributions associated with carrier-number fluctuations to the total noise spectral density. In particular, the compensation between number and velocity-number terms implies that the total noise is finally determined only by the contribution of velocity fluctuations.

In the elastic case, γ depends on the momentum space dimensionality, the suppression being less pronounced the lower the dimension of momentum space. This fact spoils the possible *universality* of the $\frac{1}{3}$ reduction found in the 3D nondegenerate case (Landauer 1998, 1999). Moreover, for a given dimensionality the consideration of an energy dependent scattering rate can also lead to different suppression factors (Beenakker 1998; Nagaev 1998*c*).

For the case of single and many barriers systems, when transport is controlled by tunneling mechanisms, we have analysed shot-noise suppression of independently transmitted electrons in semiconductor heterostructure diodes. The mechanism of suppression is based on the confinement of electrons in each well of the heterostructures due to inelastic scattering through polar-optical phonon emission, thus implying a nonuniformity of the electron flux incident on the barrier which, in turn, correlates the transmission process of electrons through the barrier. MC simulations of realistic structures confirm this model. Moreover, the results of the simulations show that shot noise is suppressed to a higher extent when the number of barriers is increased, and that the Fano factor exhibits a significant voltage dependence with a characteristic minimum value due to the non-linearity of the current–voltage characteristics. For the case of a double barrier structure, the comparison between analytical and direct MC calculations on the dependence of the Fano factor with applied voltage shows the degree of applicability of available analytical expressions. In particular, a suppression to a maximum value of $\gamma \simeq 0{\cdot}5$ has been found in close analogy with the case of a resonant structure where suppression is, however, associated with the Pauli principle. As a general trend, the presence of scattering mechanisms, especially non-elastic, is found to favour the suppression of shot noise. On the other hand, an increase of the lattice temperature is found to make suppression less significant. In all cases studied here, in the absence of any applied voltage, thermal equilibrium Johnson–Nyquist noise is obtained. This represents a valuable test of the theoretical approach and confirms the conjecture that shot noise and thermal-equilibrium noise are special forms of a more general noise formula (Stanton and Wilkins 1985; Büttiker 1986, 1992; Landauer 1989, 1993, 1998; Iannaccone and Pellegrini 1997).

Most of the calculations have been carried out for realistic structures thus opening the possibility of an experimental verification of the predicted phenomena.

Acknowledgments

This work has been performed within the Italian–Lithuanian Project 'Research and development cooperation in submicron electronics' supported by the Italian Ministery of Foreign Affairs. Partial support from the Dirección General de Enseñanza Superior e Investigación through the project PB97–1331, the Consejería de Educación y Cultura de la Junta de Castilla y León through the project SA44/99, the Physics of Nanostructures project of the Italian Ministero dell'

Universitá e della Ricerca Scientifica e Tecnologica (MURST), and the Lithuanian National Science Foundation is gratefully acknowledged.

References

Altshuler, B., Levitov, L., and Yakovets, A. (1994). *JETP Lett.* **59**, 857.
Beenakker, C. W. J. (1998). cond-mat/9810117.
Beenakker, C. W. J., and Büttiker, M. (1992). *Phys. Rev.* B **46**, 1889.
Birk, M. d. J. H., and Schönenberg, C. (1995). *Phys. Rev. Lett.* **75**, 1610.
Blanter, Y. M., and Büttiker, M. (1997). *Phys. Rev.* B **56**, 2127.
Büttiker, M. (1986). *Phys. Rev.* B **33**, 3020.
Büttiker, M. (1990). *Phys. Rev. Lett.* **65**, 2901.
Büttiker, M. (1992). *Phys. Rev.* B **46**, 12485.
Büttiker, M. (1995). *In* 'Noise in Physical Systems and $1/f$ Fluctuations' (Eds V. Bareikis and R. Katilius), p. 35 (World Scientific: Singapore).
Chen, L., and Ting, C. (1991). *Phys. Rev.* B **41**, 4534.
Chen, L., and Ting, C. (1992). *Phys. Rev.* B **46**, 4714.
Davies, J., Hyldgaard, P., Hershfield, S., and Wilkins, J. (1992). *Phys. Rev.* B **46**, 9620.
de Jong, M. (1996). *Phys. Rev.* B **54**, 8144.
de Jong, M., and Beenakker, C. W. J. (1995). *Phys. Rev.* B **51**, 16867.
de Jong, M., and Beenakker, C. (1996). *In* 'Mesoscopic Electron Transport', NATO ASI Series E (Eds L. P. Kowenhoven *et al.*), p. 225 (Plenum Kluwer: Dordrecht).
de Picciotto, R., Reznikov, M., Heiblum, M., Umansky, V., Bunin, G., and Mahalu, D. (1997). *Nature* **389**, 162.
Dorokhov, O. (1984). *Solid State Commun.* **51**, 381.
Galperin, Y., and Kozub, V. (1991*a*). *Europhys. Lett.* **15**, 631.
Galperin, Y., and Kozub, V. (1991*b*). *Sov. Phys. JETP* **73**, 179.
Gonzalez, T., and Pardo, D. (1993). *J. Appl. Phys.* **73**, 7453.
Gonzalez, T., Bulashenko, O. M., Mateos, J., Pardo, D., Reggiani, L., and Rubi, J. M. (1997*a*). *Semicond. Sci. Technol.* **12**, 1053.
Gonzalez, T., Bulashenko, O. M., Mateos, J., Pardo, D., and Reggiani, L. (1997*b*). *Phys. Rev.* B **56**, 6424.
Gonzalez, T., Gonzalez, C., Mateos, J., Pardo, D., Bulashenko, O. M., Rubi, J. M., and Reggiani, L. (1998*a*). *Phys. Rev. Lett.* **80**, 2901.
Gonzalez, T., Mateos, J., Pardo, D., Bulashenko, O. M., and Reggiani, L. (1998*b*). *Semicond. Sci. Technol.* **13**, 714.
Gonzalez, T., Mateos, J., Pardo, D., Bulashenko, O. M., and Reggiani, L. (1999). *Phys. Rev.* B **60**, 2670.
Green, F., and Das, M. (1999). cond-mat/9911251.
Hanke, U., Galperin, Y. M., Chao, K., and Zou, N. (1993). *Phys. Rev.* B **48**, 17,209.
Hershfield, S., Davies, J. H., Hyldgaard, Per, Stanton, C. J., and Wilkins, J. W. (1993). *Phys. Rev.* B **47**, 1967.
Hung, K., and Wu, G. (1993). *Phys. Rev.* B **48**, 14687.
Iannaccone, G., and Pellegrini, B. (1995). *Phys. Rev.* B **52**, 17,406.
Iannaccone, G., and Pellegrini, B. (1997). *Phys. Rev.* B **55**, 4539.
Imry, Y. (1986). *Europhys. Lett.* **1**, 249.
Jahan, M., and Anwar, A. (1995). *Solid State Electron.* **38**, 429.
Kozub, V., and Rudin, A. (1995*a*). *Phys. Rev.* B **52**, 7853.
Kozub, V., and Rudin, A. (1995*b*). *In* 'Noise in Physical Systems and $1/f$ Fluctuations' (Eds V. Bareikis and R. Katilius), p. 65 (World Scientific: Singapore).
Kubo, R., Toda, M., and Hashitsume, N. (1991). 'Statistical Physics', Vols I and II (Springer: Berlin).
Kumar, A., Saminadayar, L., Glattli, D. C., Jin, Y., and Etienne, B. (1996). *Phys. Rev. Lett.* **76**, 2778.
Lampert, M., and Mark, P. (1970). 'Curent Injection in Solids' (Academic: New York).
Landau, L., and Lifshitz, E. (1958). 'Statistical Physics' (Pergamon: Oxford).
Landauer, R. (1989). *Physica* D **38**, 226.
Landauer, R. (1993). *Phys. Rev.* B **47**, 16,427.

Landauer, R. (1996). *Physica* B **227**, 156.
Landauer, R. (1998). *Nature* **392**, 658.
Landauer, R. (1999). *Microelectron. Eng.*, in press.
Lesovik, G. B. (1989). *JETP Lett.* **49**, 592.
Li, Y. P., Tsui, D. C., Heremans, J. J., Simmons, J. A., and Weimann, G. W. (1990*a*). *Appl. Phys. Lett.* **57**, 774.
Li, Y. P., Zaslavsky, A., Tsui, D. C., Santos, M., and Shayegan, M. (1990*b*). *Phys. Rev.* B **41**, 8388.
Liefrink, F., Dijkhuis, J. I., de Jong, M. J. M., Molenkamp, W., and van Houten, H. (1994). *Phys. Rev.* B **49**, 14,066.
Liu, H., Lijianmeng, Aers, G. C., Leavens, R., Buchanan, M., and Wasilewski, Z. R. (1995). *Phys. Rev.* B **51**, 5116.
Liu, R., and Yamamoto Y. (1994). *Phys. Rev.* B **49**, 10,520.
Liu, R., Eastman, P., and Yamamoto Y. (1997). *Solid State Commun.* **102**, 785.
Liu, R., Odom, B., Yamamoto, Y., and Tarucha, S. (1998). *Nature* **391**, 263.
Lund, B., and Galperin, Y. (1997). *Phys. Rev.* B **55**, 1696.
Macucci, M., and Pellegrini, B. (1995). *In* 'Noise in Physical Systems and $1/f$ Fluctuations' (Eds V. Bareikis and R. Katilius), p. 284 (World Scientific: Singapore).
Martin, T., and Landauer, R. (1992). *Phys. Rev.* B **45**, 1742.
Moglestue, C. (1993). 'Monte Carlo Simulation of Semiconductor Devices' (Chapman Hall: London).
Nagaev, K. (1992). *Phys. Lett.* A **169**, 103.
Nagaev, K. (1995*a*). *In* 'Noise in Physical Systems and $1/f$ Fluctuations' (Eds V. Bareikis and R. Katilius), p. 53 (World Scientific: Singapore).
Nagaev, K. (1995*b*). *Phys. Rev.* B **52**, 4740.
Nagaev, K. (1998*a*). *Phys. Rev.* B **57**, 4628.
Nagaev, K. (1998*b*). *Phys. Rev.* B **58**, R7512.
Nagaev, K. (1998*c*). cond-mat/9812317.
Naveh, Y., Averin, D., and Likharev, K. (1997). *Phys. Rev. Lett.* **79**, 3482.
Nazarov, Y. V. (1994). *Phys. Rev. Lett.* **73**, 134.
Pellegrini, B. (1986). *Phys. Rev.* B **34**, 5921.
Pellegrini, B. (1993*a*). *Nuovo Cimento* **15**, 855.
Pellegrini, B. (1993*b*). *Nuovo Cimento* **15**, 881.
Ramo, S. (1939). *Proc. IRE* **27**, 584.
Reggiani, L., Kuhn, T., and Varani, L. (1992). *App. Phys.* **54**, 411.
Reklaitis, A. (1996*a*). Proc. 3rd ELEN Workshop, Leuven, Belgium (Eds C. Clayes and E. Simoen), p. 108 (IMEC: Leuven, Belgium).
Reklaitis, A. (1996*b*). *J. Appl. Phys.* **80**, 1242.
Reklaitis, A., and Reggiani, L. (1997*a*). *J. Appl. Phys.* **82**, 3161.
Reklaitis, A., and Reggiani, L. (1997*b*). *Phys. Stat. Sol. (b)* **204**, 459.
Reklaitis, A., and Reggiani, L. (1999). *Semicond. Sci. Technol.* **14**, 15.
Reznikov, M., Heiblum, M., Shtrikman, H., and Mahalu, D. (1995). *Phys. Rev. Lett.* **75**, 3340.
Saminadayar, L., Glattli, D., Jin, Y., and Etienne, B. (1997). *Phys. Rev. Lett.* **79**, 2526.
Schep, K., and Bauer, G. (1997). *Phys. Rev. Lett.* **78**, 3015.
Schoelkopf, R., Burke, P. J., Kozhevnikov, A. A., Prober, E., and Rooks, M. J. (1997). *Phys. Rev. Lett.* **78**, 3370.
Schottky, W. (1918). *Ann. Phys. (Leipzig)* **57**, 541.
Sheng, H., and Chua, S.-J. (1994). *J. Phys.* D **27**, 137.
Shimizu, A. and Ueda, M. (1992). *Phys. Rev. Lett.* **69**, 1403.
Shimizu, A., Ueda, M., and Sakaki, H. (1992). Workshop on Quantum Effects, Luxor Inst. Phys. Conf. Ser. No. 217, Chapt. 2, p. 29, Kyoto.
Shockley, W. (1938). *J. Appl. Phys.* **9**, 635.
Stanton, C. J., and Wilkins, J. W. (1985). *Physica* **134B**, 255.
Steinbach, A. H., Martinis, J. M., and Devoret, M. H. (1996). *Phys. Rev. Lett.* **76**, 3806.
Sukhorukov, E., and Loss, D. (1998). *Phys. Rev. Lett.* **80**, 4959.
Thompson, B., North, D., and Harris, W. A. (1940*a*). *RCA Review* **4**, 269.
Thompson, B., North, D., and Harris, W. A. (1940*b*). *RCA Review* **4**, 441.

van de Roer, T., Heyer, H., and Kwaspen, J. (1991). *Electron. Lett.* **27**, 2158.
van der Ziel, A. (1954). 'Noise' (Prentice-Hall: New York).
van der Ziel, A. (1986). 'Noise in Solid State Devices and Circuits' (Wiley: New York).
Varani, L., Reggiani, L. Kuhn, T., Gonzalez, T., and Pardo, D. (1994). *IEEE Trans. Electron Dev.* **41**, 1916.
Yan, S., Edwards, B. S. H. P., and Lynam, P. (1997). *Phys. Rev.* B **55**, 12,880.
Yurke, B., and Kochanski, G. (1990). *Phys. Rev.* B **41**, 8184.

Manuscript received 30 March, accepted 22 June 1999